



ELSEVIER

European Journal of Radiology 44 (2002) 52–58

EJR
EUROPEAN JOURNAL OF RADIOLOGY

www.elsevier.com/locate/ejrad

Differentiation of prostate cancer from benign prostate hypertrophy using dual-echo dynamic contrast MR imaging

Satoshi Muramoto ^{a,*}, Hidemasa Uematsu ^a, Hirohiko Kimura ^a, Yoshiyuki Ishimori ^a, Norihiro Sadato ^b, Nobuyuki Oyama ^c, Tsuyoshi Matsuda ^d, Yasutaka Kawamura ^a, Yoshiharu Yonekura ^e, Kenichiro Okada ^c, Harumi Itoh ^a

^a Department of Radiology, Fukui Medical University, 23 Shimoaizuki, Matsuoka, Yoshida, Fukui 910-1193, Japan

^b Psychophysiology Section, Department of Cerebral Research, National Institute for Physiological Sciences, Aichi, Japan

^c Department of Urology, Fukui Medical University, Fukui, Japan

^d Application Research Department, Advanced Technology Center, GE Yokogawa Medical Systems Ltd., Tokyo, Japan

^e Biomedical Imaging Research Center, Fukui Medical University, Fukui, Japan

Received 5 November 2001; received in revised form 6 November 2001; accepted 7 November 2001

Abstract

Objective: To investigate the usefulness of dynamic contrast magnetic resonance (MR) imaging in the differentiation of prostate cancer (PC) from benign prostate hypertrophy (BPH). **Materials and methods:** Eleven PC patients and 13 BPH patients were entered into the analysis. The mean gradient (MG) was calculated from the T2* term-eliminated time-signal intensity curve obtained from dynamic contrast MR data, and the MG of PC and that of BPH were compared. **Results:** The MG of PC was significantly higher than that of BPH. When the threshold value was set to 1.88% per s for discriminating PC from BPH, the sensitivity, specificity, and accuracy were 100, 85, and 92%, respectively. **Conclusion:** The MG, which is derived from the T2* term-eliminated time-signal intensity curve, may be a useful index for differentiating PC from BPH. © 2002 Elsevier Science Ireland Ltd. All rights reserved.

Keywords: MR-imaging; Urinary; Prostate; Neoplasms-primary; Tissue characterization

1. Introduction

Magnetic resonance (MR) imaging is a practical method for staging patients with prostate cancer (PC), and is helpful for selecting patients with surgically resectable disease [1–3]. It is very important to identify and localize the tumors accurately within prostate tissue, because, this information allows investigators to more accurately evaluate transcapsular tumor spread and tumor staging. The evaluation of tumor volume is also clinically important, because, tumor volume is related to metastasis, seminal vesicle invasion, and histological differentiation [4]. Most PC occurs in the peripheral zone (PZ), which is delin-

eated as an abnormally low signal intensity area surrounded by the high signal intensity of the PZ on T2-weighted spin echo (SE) images. However, the usefulness of T2-weighted images is limited, because, as many as 30% of PC occur within the central gland (CG), the signal intensity of which is similar to that of PC [1]. Gadolinium enhanced T1-weighted SE images do not provide information more useful than that on T2-weighted SE images, except in detecting seminal vesicle and neuro-vascular bundle involvement [5,6].

Although, PC is not a macroscopic hypervascular tumor that is easily depicted on conventional angiography or computed tomography (CT) with bolus injection of iodinated contrast agent, microvessel density is higher in PC than in benign prostate tissue in the pathological analysis [7,8]. Therefore, to investigate, whether differential diagnosis between benign prostate hypertrophy (BPH) and PC can be made

* Corresponding author. Tel.: +81-776-61-3111x2335; fax: +81-776-61-8137.

E-mail address: muramoto@fmsrsa.fukui-med.ac.jp (S. Muramoto).

using imaging modalities, a study was conducted in which quantitative measurement of blood flow in prostate lesions was attempted using positron emission tomography with $H_2^{15}O$ [9]. This study demonstrated that the regional blood flow of PC was significantly higher than that of BPH, and showed potential for use in differentiating between PC and BPH. However, positron emission tomography requires a cyclotron for the production of a tracer with an extremely short half-life (2-min). Furthermore, arterial input function from an artery is necessary to calculate the absolute regional blood flow. Therefore, a complementary approach by MR imaging may be useful in differentiating prostate lesions in clinical settings.

T1-weighted dynamic MR imaging with contrast agent has been utilized for the characterization of tissue types in several organs [10–13]. The early signal enhancement effect has been used to determine the degree of tumor vascularization [10–14]; increase in contrast agent uptake may reflect neovascularization in malignant tissue. To date, several dynamic MR studies in the prostate region have been reported [15–17]. In these studies, the early signal enhancement using dynamic MR images demonstrated clearer delineation of the extension of malignant tumors compared with conventional SE images, thus resulted in improved staging results [15,16]. However, similar early signal enhancement is frequently observed in the CG of BPH; therefore, findings from previous dynamic studies turned out to be insufficient for purposes of differentiating between PC and BPH [15–17].

After bolus injection, a contrast agent such as, gadopentetate dimeglumine (Gd-DTPA) causes a T1 shortening effect when it leaks into the interstitial space. On the other hand, contrast agent remaining in the vascular space causes a signal decrease as a result of the increased heterogeneity of local magnetic fields ($T2^*$ shortening effect). In a normal brain with intact blood–brain barriers, the dominant $T2^*$ shortening effect occurs; however, in PC, the T1 and $T2^*$ shortening effects occur simultaneously. Therefore, in previous studies [15–17], the MR signal after the bolus injection of the contrast agent was partially cancelled out by its $T2^*$ shortening effect, due to the presence of intravascular contrast agent in the prostate tissues. If this $T2^*$ shortening effect could be removed from the MR signal, a stronger relationship would exist between the MR signal and the concentration of the contrast agent. Dual-echo dynamic contrast MR imaging can provide the correct T1 signal change by eliminating the $T2^*$ shortening effect [18]. In this study, our aim was to investigate the usefulness of this T1 signal change for differentiating between PC and BPH.

2. Materials and methods

2.1. Theory

After bolus injection, Gd-DTPA causes a T1 shortening effect due to the leakage of contrast agent into permeable tissue that is partially cancelled by $T2^*$ shortening caused by the intravascular contrast agent. The relationship between the signal intensity of a gradient echo sequence and the relaxation time can be expressed as follows:

Signal intensity

$$= \beta \frac{[1 - \exp(-TR/T1)] \exp(-TE/T2^*) \sin \alpha}{1 - \exp(-TR/T1) \cos \alpha} \quad (1)$$

where β is the scaling factor, TR the repetition time, TE the echo time, and α the flip angle. The $T2^*$ term consists of $\exp(-TE/T2^*)$. If the $T2^*$ value (not the $T2^*$ term) is given in Eq. (1), the $\exp(-TE/T2^*)$ is eliminated from the signal intensity as described in Eq. (1). The $T2^*$ rate ($1/T2^*$) is calculated from the dual-echo MRI data as follows [18,19]:

$$\frac{1}{T2^*} = \ln \left[\frac{S(TE1)/S(TE2)}{TE2 - TE1} \right] \quad (2)$$

where $S(TE1)$ and $S(TE2)$ represent the signal intensity of the first TE and the second TE, respectively. After the $T2^*$ term is eliminated in Eq. (1), the MR signal is considered to have a stronger relationship with the concentration of the contrast agent.

2.2. Subjects

Thirty-four consecutive patients were investigated in this study. These patients included two groups, as follows, the first consisted of pathologically confirmed PC patients; the second of patients who had suspiciously high levels of serum prostate specific antigen, and underwent MR studies to determine the presence of PC. Ten patients were excluded from the analysis for the following reasons, significant artifact due to rectal distension ($n = 7$); or unstable time-signal intensity curves resulting from the small size of the lesions ($n = 3$). Eleven patients with PC (age range, 60–85 years; mean age, 75.0 years) and 13 patients with BPH (age range, 44–79 years; mean age, 68.9 years) were entered into the final analysis. In seven of 13 BPH patients, normal PZ was not observed as a homogeneous high signal intensity on T2-weighted FSE images, because of significant hypertrophy of the CG; therefore, regions of interest (ROIs) for PZ were analyzed in the remaining six of the 13 BPH patients. The institutional review board approved the study, and informed consent was obtained from all patients

before the MR study. Final pathological diagnoses of all patients were confirmed by histopathological specimens.

2.3. MR technique

MR studies and biopsies were performed within 6 weeks. If the biopsy was completed prior to the MR study, the MR study was performed at least 3 weeks after the biopsy to minimize post-operative effects such as hemorrhage. All MR images were obtained with a 1.5 T clinical MR imaging system (Horizon, General Electric Medical Systems, Milwaukee, WI, USA). The phased-array coils provided by the manufacturer were used for all experiments. After coronal T2-weighted localizing fast SE (FSE) images (TR/TE/number of excitations (NEX)/echo train length: 3000 ms/85.8 ms/2/16) were obtained, sagittal (3800/82.2/4/16) and axial (3700/84.5/4/16) T2-weighted FSE images and axial T1-weighted SE images (450/9/2) were also acquired. The imaging parameters for all image sequences were as follows: matrix size: 256×256 ; slice thickness: 4 mm; slice gap: 1 mm; field of view (FOV): 24×24 cm.

The single section in which the tumor was most likely to be present was selected from the T2-weighted FSE images. An irregular area of low signal intensity in the PZ and low signal intensity in the periprostatic fat with a disruption of the prostatic capsule on the T2-weighted FSE images were considered to indicate PC. If no apparent tumor was observed, another section was selected from the T2-weighted FSE images in which both the CG and PZ were most likely to be present. In

this section, we used single section spoiled gradient recalled acquisition (SPGR) images (TR/TE1, TE2/NEX/flip angle: 33.3/7, 20/0.75, 10°; matrix size: $256 \times 128 - 96$; slice thickness: 7 mm; rectangular FOV: 24×16 cm). Ten seconds after the start of dynamic SPGR imaging, 0.1 mmol/kg body weight of Gd-DTPA (Magnevist, Nihon Schering, Osaka, Japan) was rapidly injected at a rate of 4 ml/s with an MR-compatible power injector (MRS-50, Nemoto, Tokyo, Japan), followed by a 20-ml saline flush. Sequential dynamic images were obtained every 1.85–2.45 s for 2.5 min. After the dynamic studies, T1-weighted axial and coronal SE images were also obtained.

2.4. Data analysis

For quantitative analysis, we calculated the following two indexes from ROIs analysis to characterize the tissue from the time–signal intensity curve derived from Eqs. (1) and (2) as described in the Section 2.1: maximum percent signal change and mean gradient (MG). All ROIs were determined on the SPGR images by one radiologist (S.M.). ROIs for PC were determined by referring to the T2-weighted FSE images, transrectal ultrasonography, and biopsy results. The areas considered to be necrotic tissue, which showed a lack of signal enhancement on gadolinium enhanced T1-weighted SE images or significant high signal intensity indicating fluid on T2-weighted FSE images, were excluded from the ROIs. When a radical prostatectomy was performed, MR images were correlated to gross histopathological specimens. In each BPH patient, a ROI

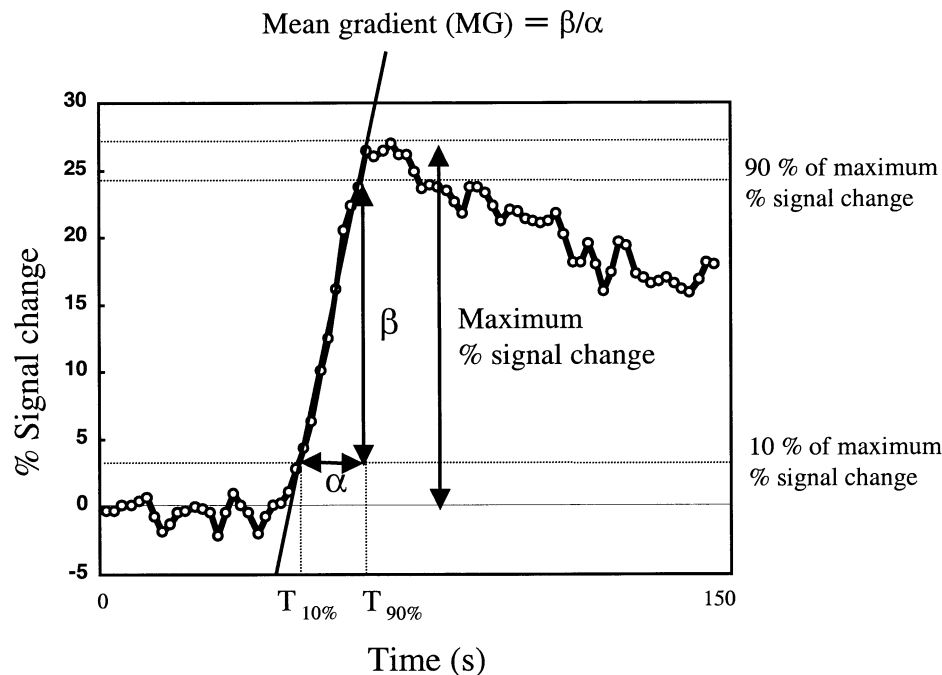


Fig. 1. Time T2* term-eliminated percent signal change curve. Maximum percent signal change and MG are defined as shown.

was determined in the CG and PZ, respectively. ROIs for PZ were determined in the areas showing high signal intensity on corresponding T2-weighted FSE images. As shown in Fig. 1, the maximum percent signal change was defined as the peak level of percent signal change during the dynamic measurement period. The MG was defined as the average rate of percent signal change between 10 and 90% of maximum percent signal change.

Parametric maps for maximum percent signal changes

and MG were created for each subject for purposes of visual assessment. We did not place the ROIs on the parametric maps, due to the relatively low signal-to-noise ratios of the original dynamic images. MR images were transferred to a workstation (Ultra 1 creator 313; Sun Microsystems, Mountain View, CA, USA). On a pixel-by-pixel basis, the signal intensity was converted into the T2* term-eliminated percent signal change. These maps were generated by in-house software.

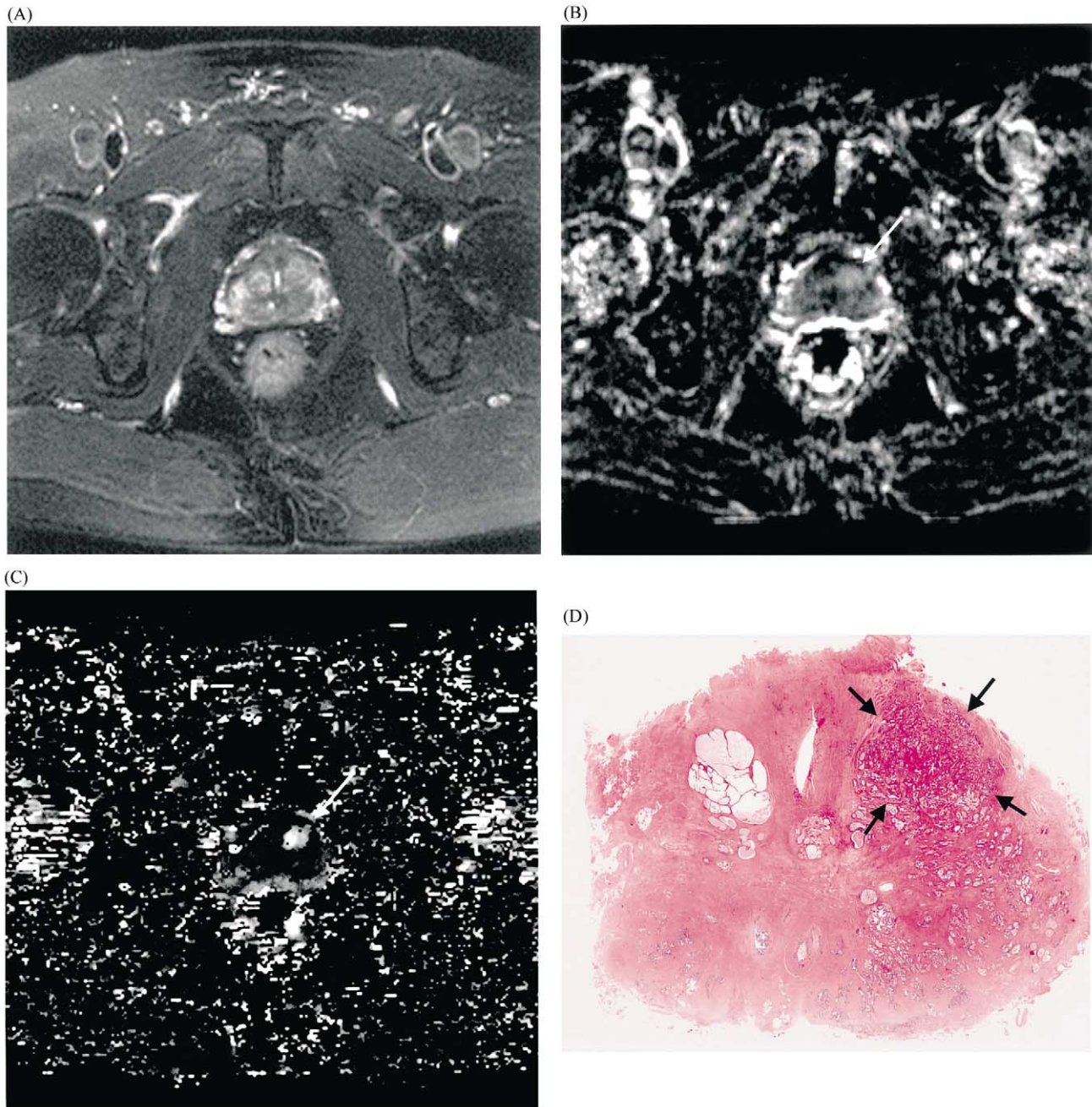


Fig. 2. A 60-year-old man with PC. (A) No apparent tumor can be seen in the prostate on the T2-weighted FSE image. (B) High intensity area is seen in the left CG on the corresponding maximum percent signal change map (white arrow). (C) High intensity area is seen in the left CG on the corresponding MG map (white arrow). (D) Histopathological specimen obtained at a corresponding level reveals the PC (black arrows) in the left CG. Tumor size was 8 × 6 mm. Hematoxylin-eosin staining; original magnification.

2.5. Statistical analysis

The data were then examined for differences between various tissue types. $P < 0.05$ was considered to be statistically significant using the non-parametric Mann–Whitney U -test.

3. Results

The typical PC was characterized by a high maximum percent signal change, and a high MG (Fig. 2). On the other hand, the typical CG and PZ of BPH were characterized by a relatively low maximum percent signal change, and a low MG (Fig. 2). In one patient, a PC within CG was detected on the parametric map, which was not visualized on T2-weighted FSE image (Fig. 2).

The values of maximum percent signal change (mean \pm S.D.) in CG, PZ, and PC were 22.3 ± 4.8 , 18.5 ± 3.4 , and $26.5 \pm 7.8\%$, respectively. The values of maximum percent signal change of PC was statistically higher than that of CG ($P < 0.02$) and PZ ($P < 0.03$); however, there was significant overlap between them (Fig. 3a).

The values of MG in CG, PZ, and PC were 1.21 ± 0.67 , 0.63 ± 0.28 , and $2.90 \pm 0.91\%$ per s, respectively. The values of the MG of PC were statistically higher than those of the CG ($P < 0.0003$) and the PZ ($P < 0.001$). When the threshold value was set to 1.88% per s to discriminate PC from BPH, the sensitivity, specificity, and accuracy were 100, 85, and 92%, respectively (Fig. 3b).

4. Discussions and conclusion

This MR study demonstrated that the MG was useful for differentiation between PC and BPH. The contrast agent uptake rate of the dynamic study has been proven to be directly proportional to the degree of microvessel density [10–14]. In this study, the MG was considered to be an important parameter representing the vascularity of tissue, because, it was equivalent to the contrast agent uptake rate. Considered a means of evaluating the induction of new vessels by malignant tissue, the MG allowed for successful differentiation between PC and BPH.

Maximum percent signal change is also considered to be an important index to represent the vascularization of tissue. Although, we found a significant difference between the maximum percent signal change of PC and CG of BPH ($P < 0.02$), and between the maximum percent signal change of PC and PZ of BPH ($P < 0.03$), there was considerable overlap between them. Assuming that the permeability of capillaries and leakage

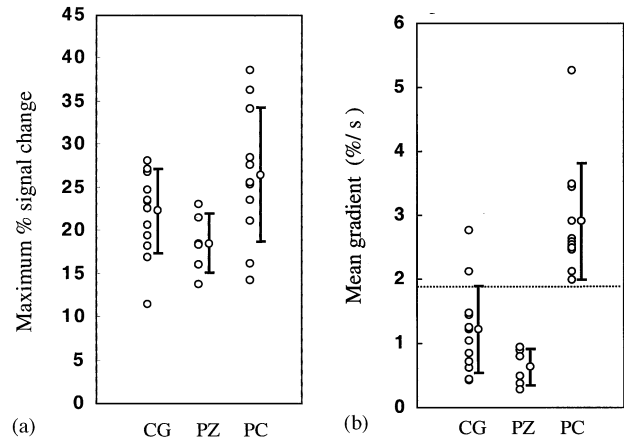


Fig. 3. (a) Scatter plot of maximum percent signal change is shown for CG, PZ, and PC. The mean and S.D. are also shown. The values of maximum percent signal change of PC are statistically higher than those of CG ($P < 0.02$) and PZ ($P < 0.03$); however, there is significant overlap between them. (b) Scatter plot of MG is shown using the same format as that in (a). The values of MG of PC are statistically higher than those of CG ($P < 0.0003$) and PZ ($P < 0.001$). When the threshold value of the MG is set to 1.88% per s to discriminate PC from benign prostate tissue, the sensitivity, specificity, and accuracy are 100, 85, 92%, respectively. The MG cutoff (% per s) for discrimination from PC is indicated by the broken line.

space are equal between lesions, contrast agent accumulation after the first pass of contrast agent becomes higher in proportion to the vascularity of tissues. However, because, signal enhancement represents the total contrast agent uptake in the tissue, maximum signal enhancement also depends on the volume of the leakage space; therefore, the maximum signal enhancement will not represent the vascularity itself. Therefore, the MG is suggested to be an index more accurate than maximum percent signal change for representing the vascularity.

In previous reports, several parameters have been proposed to characterize the MR signal intensity curves of prostate lesions [15–17,20]. It is very important to differentiate the signal enhancement of PC and that of BPH, because, PC is frequently accompanied by BPH. However, no significant difference was found in any parameters between PC and BPH [15–17,21], except in one previous report that examined intra-patient difference [20]. Although, BPH is a benign proliferative process, increased microvessel density comparable with that of cancers has been reported in some cases of BPH [22]; therefore, it is difficult to differentiate between the two types of lesions.

In this study, a PC, within CG was detected on the parametric maps, which was not visualized on T2-weighted FSE image (Fig. 2). While the PC in PZ is easily delineated on T2-weighted SE images, the usefulness of T2-weighted images is limited, because, as many as 30% of PC occur within the CG (CG), the signal

intensity of which is similar to that of PC [1]. The MG maybe a useful adjunct for the differentiation of PC from benign prostate tissue within CG.

In the present study, T2* correction was sufficient for the exact evaluation of contrast agent uptake in the tissue. After the rapid injection of intravascular contrast agent, the T2* shortening effect was more than negligible even in the relatively short TE MR imaging (TE = 7 ms). During this period, the linear relationship between T1 rate change ($\Delta I/I$) and contrast agent concentration may break down. After the first pass of contrast agent, the roles are reversed and the T1 shortening effect becomes the stronger effect. Therefore, contrast agent accumulation at the early phase of signal enhancement is likely to be underestimated, especially in hypervascular tissue. Consequently, the T2* effect must be corrected in order to obtain precise evaluation of contrast agent uptake in dynamic MR study.

In this study, the temporal resolution of a dynamic image was about 2 s, which was shorter than that in recent dynamic studies [15,17]. The MR signal changes rapidly during the first pass of the contrast agent after bolus injection. In this study, the majority of signal increase was observed within approximately 10 s from the initial increase of the signal intensity curve. Therefore, for the precise evaluation of contrast agent uptake at the early phase of dynamic study, higher temporal resolution is needed. Although, Jager et al. [3] performed single slice fast dynamic MR imaging without T2* correction at a high temporal resolution of 1.25 and 2.5 s, they failed to differentiate between benign and malignant prostate tissues. We speculate that their simple classification of the signal enhancement curve into three categories may have led to unexpected results, because, the difference in signal enhancement patterns between PC and BPH is very small.

In conclusion, the MG, which was derived from the time–MR signal intensity curve with the elimination of the T2* term, may be a useful index for the differentiation of PC from benign prostate tissue in the clinical setting.

Acknowledgements

This study was supported in part by a research grant (JSPS-RFTF97L00203) from the Japan Society for the Promotion of Science. The authors thank Hiroto Hatabu, Hiroki Yamada, and Yoshio Koshimoto, for their useful discussion; Hiroyuki Sashie, Tomokazu Ishida, and Miho Takeuchi, for their assistance with MRI data collection, and Lorene M. Yoxthimer, for her assistance with manuscript preparation.

References

- [1] Schiebler ML, Schnall MD, Pollack HM, Lenkinski RE, Tomaszewski JE, Wein AJ, Whittington R, Rauschnig W, Kressel HY. Current role of MR imaging in the staging of adenocarcinoma of the prostate. *Radiology* 1993;189:339–52.
- [2] D'Amico AV, Whittington R, Schnall M, Malkowicz SB, Tomaszewski JE, Schultz D, Wein A. The impact of the inclusion of endorectal coil magnetic resonance imaging in a multivariate analysis to predict clinically unsuspected extraprostatic cancer. *Cancer* 1995;75:2368–72.
- [3] Jager GJ, Ruijter ET, van de Kaa CA, de la Rosette JJ, Oosterhof GO, Thornbury JR, Barentsz JO. Local staging of prostate cancer with endorectal MR imaging: correlation with histopathology. *Am J Roentgenol* 1996;166:845–52.
- [4] McNeal JE, Bostwick DG, Kindrachuk RA, Redwine EA, Freiha FS, Stamey TA. Patterns of progression in prostate cancer. *Lancet* 1986;1:60–3.
- [5] Mirowitz SA, Brown JJ, Heiken JP. Evaluation of the prostate and prostatic carcinoma with gadolinium-enhanced endorectal coil MR imaging. *Radiology* 1993;186:153–7 see comments.
- [6] Huch Boni RA, Boner JA, Lutolf UM, Trinkler F, Pestalozzi DM, Krestin GP. Contrast-enhanced endorectal coil MRI in local staging of prostate carcinoma. *J Comput Assist Tomogr* 1995;19:232–7.
- [7] Brawer MK, Bigler SA, Deering RE. Quantitative morphometric analysis of the microcirculation in prostate carcinoma. *J Cell Biochem Suppl* 1992;16H:62–4.
- [8] Bigler SA, Deering RE, Brawer MK. Comparison of microscopic vascularity in benign and malignant prostate tissue. *Hum Pathol* 1993;24:220–6.
- [9] Inaba T. Quantitative measurements of prostatic blood flow and blood volume by positron emission tomography. *J Urol* 1992;148:1457–60.
- [10] Nagele T, Petersen D, Klose U, Grodd W, Opitz H, Gut E, Martos J, Voigt K. Dynamic contrast enhancement of intracranial tumors with SNAPSHOT-FLASH MR imaging. *Am J Neuroradiol* 1993;14:89–98.
- [11] Hulka CA, Smith BL, Sgroi DC, Tan L, Edmister WB, Semple JP, Campbell T, Kopans DB, Brady TJ, Weisskoff RM. Benign and malignant breast lesions: differentiation with echo-planar MR imaging. *Radiology* 1995;197:33–8.
- [12] Buadu LD, Murakami J, Murayama S, Hashiguchi N, Sakai S, Masuda K, Toyoshima S, Kuroki S, Ohno S. Breast lesions: correlation of contrast medium enhancement patterns on MR images with histopathologic findings and tumor angiogenesis. *Radiology* 1996;200:639–49.
- [13] Hulka CA, Edmister WB, Smith BL, Tan L, Sgroi DC, Campbell T, Kopans DB, Weisskoff RM. Dynamic echo-planar imaging of the breast: experience in diagnosing breast carcinoma and correlation with tumor angiogenesis. *Radiology* 1997;205:837–42.
- [14] van der Sanden BP, Rozijn TH, Rijken PF, Peters HP, Heerschap A, van der Kogel AJ, Bovee WM. Noninvasive assessment of the functional neovasculature in 9L-glioma growing in rat brain by dynamic IH magnetic resonance imaging of gadolinium uptake. *J Cereb Blood Flow Metab* 2000;20:861–70.
- [15] Brown G, Macvicar DA, Ayton V, Husband JE. The role of intravenous contrast enhancement in magnetic resonance imaging of prostatic carcinoma. *Clin Radiol* 1995;50:601–6.
- [16] Jager GJ, Ruijter ET, van de Kaa CA, de la Rosette JJ, Oosterhof GO, Thornbury JR, Ruijs SH, Barentsz JO. Dynamic TURBOFLASH subtraction technique for contrast-enhanced MR imaging of the prostate: correlation with histopathologic results. *Radiology* 1997;203:645–52.

- [17] Padhani AR, Gapinski CJ, Macvicar DA, Parker GJ, Suckling J, Revell PB, Leach MO, Dearnaley DP, Husband JE. Dynamic contrast enhanced MRI of prostate cancer: correlation with morphology and tumour stage, histological grade and PSA. *Clin Radiol* 2000;55:99–109.
- [18] Uematsu H, Maeda M, Sadato N, Matsuda T, Ishimori Y, Koshimoto Y, Yamada H, Kimura H, Kawamura Y, Matsuda T, Hayashi N, Yonekura Y, Ishii Y. Vascular permeability: quantitative measurement with double-echo dynamic MR imaging—theory and clinical application. *Radiology* 2000;214:912–7.
- [19] Miyati T, Banno T, Mase M, Kasai H, Shundo H, Imazawa M, Ohba S. Dual dynamic contrast-enhanced MR imaging. *J Magn Reson Imaging* 1997;7:230–5.
- [20] Turnbull LW, Buckley DL, Turnbull LS, Liney GP, Knowles AJ. Differentiation of prostatic carcinoma and benign prostatic hyperplasia: correlation between dynamic Gd-DTPA-enhanced MR imaging and histopathology. *J Magn Reson Imaging* 1999;9:311–6.
- [21] Barentsz JO, Engelbrecht M, Jager GJ, Witjes JA, de LaRosette J, van Der Sanden BP, Huisman FU, Heerschap A. Fast dynamic gadolinium-enhanced MR imaging of urinary bladder and prostate cancer. *J Magn Reson Imaging* 1999;10:295–304.
- [22] Deering RE, Bigler SA, Brown M, Brawer MK. Microvasculature in benign prostatic hyperplasia. *Prostate* 1995;26:111–5.